Microscopic effective charges and quadrupole moments of *sd*-shell and *sd-pf* cross-shell nuclei with Z≥13

R.A. Radhi, A. H. Ali

Department of Physics, College of Science, University of Baghdad, Baghdad, Iraq

E-mail: ah70med15@gmail.com

Abstract

Effective charges of electric quadrupole moments are calculated for *sd* and cross *sd-pf* shell isotopes with $Z \geq 13$. Perturbation theory of one-particle one hole with $2\hbar\omega$ excitation is employed. Shell-model in the *sd* valence space is used for neutron number $N \leq 20$. For neutron rich nuclei with $N > 20$, *sdpf* valence space is used with full *sd* shell (Z-8) protons and full *pf* shell (N-20) neutrons. Good agreement is obtained with the measured data for most of the isotopes considered in this work while it deteriorates for some of them and need further investigation.

Key words

Effective charges and quadrupole moments of sd- and sdpf-shell isotopes (Z≥13): sd and sdpf- shell model, core-polarization effects.

Article info.

Received: Apr. 2016
Accepted: May. 2016
Published: Sep. 2016

الشحنات الفعالة المجهرية وعزوم رباعية القطب لقشرة *sd* وتقاطع قشرة *sdpf* لنوى Z≥13

رعد عبدالكريم راضي، احمد حسين علي

قسم الفيزياء كلية العلوم، جامعة بغداد، بغداد، العراق

الخلاصة

حسبت الشحنات الفعالة وعزوم رباعية القطب الكهربائية لنظائرقشرة *sd* و تقاطع *sd-pf* لنظائر ذات الاعداد الذرية الاكبر او يساوي 13. استخدمت نظرية الاضطراب من جسيم –فجوه مع طاقة تهيج $2\hbar\omega$. استخدم فضاء قشرة تكافؤ *sd* لعدد نيوترونات الاصغر او يساوي 20. اما للنوى الغنية بالنيوترونات ذات عدد نيوترونات اكبر من 20، استعمل فضاء تكافؤ *sd-pf* للنيوترنات وفضاء تكافؤ القشرة *sd* ممتلئ للبروتونات (Z-8). حصلت توافقات جيدة مع البيانات المقاسة لأغلب النظائر المفترضة في هذا العمل بينما يتباين التوافق للبعض منها وتحتاج الى مزيد من التحقق والبحث.

Introduction

The nuclear quadrupole moment, is considered as a probe for the deviation of nuclear charge from spherical symmetry. The available experimental quadrupole moment data for *sd* shell nuclei are fundamental tools for describing microscopic theories and nuclear structure studies in this mass region. Neutron-rich nuclei far from stability line provide an attractive testing ground of nuclear structure studies. They have been extensively investigated because their exotic properties which are different from those of stable nuclei. Moving away from stability line, revealed that the N = 28 shell gap is eroded in spite of the magic character for other nuclei near the stability line. Recent theoretical and experimental studies [1-3] show a direct evidence of collapse of N = 28 shell closure. Full *sd*-shell calculations are possible for neutron-rich *sd*-shell

nuclei with $N \leq 20$. For $N > 20$, *sdpf* model space is required in this case. However, full *sdpf* is not possible, so the valence (active) protons are restricted to the *sd* shell and $N > 20$ neutrons to the *pf* shell. The 20 neutrons are frozen in *s*, *p* and *sd*-shells. For electric quadrupole moment calculations, model space wave functions alone cannot describe such collective features, and one needs to renormalize the matrix elements to get a satisfactory description of the experimental data. The conventional approach to supplying this added ingredient to shell model wave functions is to redefine the properties of the valence nucleons from those exhibited by actual nucleons in free space to model effective values [4]. Effective charges are introduced to take into account effects of model-space truncation. A systematic analysis has been made for observed $B(E2)$ values with shell-model wave functions using a least-squares fit with two free parameters gave standard proton and neutron effective charges, $e_{\mathrm{p}}^{\mathrm{eff}} = 1.3e$ and $e_{\mathrm{n}}^{\mathrm{eff}} = 0.5e$ [5], in *sd*-shell nuclei. The least-square fit for the effective charges for *sd*-shell nuclei from $A = 17$ to $A = 39$ gave essentially the same results for USD, USDA and USDB Hamiltonians: e_p= 1.36(5)*e* and e_n= 0.45(5)*e* [6]. Rydt et al. [7] showed that the proton effective charge 1.1*e* obtained by a comparison of measured quadrupole moments of odd-*Z* even-*N* with shell-model calculations provides a much better description of nuclear properties in the *sd*-shell than the standard value 1.3*e*.

In spite of the need of these effective charges to renormalize the matrix elements, several discrepancies between theory and experiment are revealed, triggering the need for further experimental and theoretical researches and a revision of the effective charges [8]. One particle- one hole excitations of the core and model space provide a more practical and theoretical alternative for calculating nuclear collectivity. These effects are essential in describing transitions involving collective modes such as E2 transition between states in the ground state rotational band, such as in ^{18}O[9]. The quadrupole moment gives a useful measure of how the core is polarized especially if the valence nucleons are neutrons which do not directly participate to the electric quadrupole moment. Quadrupole moments and effective charges are calculated [10] for Li (A = 7, 8, 9, 11) and B (A = 8, 10, 11, 12, 13, 14, 15) isotopes based on the shell model including core-polarization effect, which agree very well with the experimentally observed trends of the recent experimental data.

A review of the ground state quadrupole moments for the entire *sd*-shell nuclei has been presented and compared to shell-model calculations using standard effective charges [3].

In the present work, we will adopt shell model calculations with a harmonic oscillator (HO) and Woods-Saxon (WS) single particle wave functions to calculate the quadrupole (Q) moments of *sd* and cross *sd-pf* shell nuclei with Z ≥ 13. One particle-one hole (1p–1h) excitations from the core and model space will be taken into consideration through first-order perturbation theory.

Theory

The one-body electric multipole transition operator with multipolarity J for a nucleon is given by

$$\hat{O}_{JM}(\vec{r})_k = r_k^J Y_{JM}(\Omega_k), \qquad (1)$$

The electric quadrupole moment in a state $|JM = 0>$ is [11]

$$Q(J=2)=\begin{pmatrix} J_i & 2 & J_i \\ -J_i & 0 & J_i \end{pmatrix}\sqrt{\frac{16\pi}{5}}\left\langle J_i \| \sum_k e(k)\hat{O}_{J=2,M=0}(\vec{r})_k \| J_i \right\rangle \quad (2)$$

where $e(k)$ is the electric charge for the k-th nucleon. Since $e(k)$ = 0 for neutron, there should appear no direct contribution from neutrons; however, this point requires further attention: The addition of a valence neutron will induce polarization of the core into configurations outside the adopted model space. Such core polarization effect is included through perturbation theory which gives effective charges for the proton and neutron. The Q moment can be written in terms of the proton and neutron contributions

$$Q(J=2)=\begin{pmatrix} J_i & 2 & J_i \\ -J_i & 0 & J_i \end{pmatrix}\sqrt{\frac{16\pi}{5}}\sum_{t_z} e(t_z)\left\langle J_i \| \hat{O}_2(\vec{r},t_z) \| J_i \right\rangle , \quad (3)$$

where t_z = 1/2 for a proton and t_z = -1/2 for a neutron and $\left\langle J_i \| O_2(\vec{r},t_z) \| J_i \right\rangle$ is the J = 2 electric matrix element which is expressed as the sum of the products of the one-body density matrix (OBDM) times the single-particle matrix elements,

$$\left\langle J_i \| \hat{O}_2(\vec{r},t_z) \| J_i \right\rangle = \sum_{jj'} OBDM(J_i, J=2, t_z, j, j')\left\langle j \| \hat{O}_2(\vec{r},t_z) \| j' \right\rangle , \quad (4)$$

where j and j' label single-particle states for the shell model space.

The role of the core and the truncated space can be taken into consideration through a microscopic theory, which combines shell model wave functions and configurations with higher energy as first order perturbation to describe EJ excitations: these are called core polarization effects. The reduced matrix elements of the electron scattering operator is expressed as a sum of the model space (MS) contribution and the core polarization (CP) contribution, as follows:

$$Q(J=2)=\begin{pmatrix} J_i & 2 & J_i \\ -J_i & 0 & J_i \end{pmatrix}\sqrt{\frac{16\pi}{5}}\sum_{t_z}\left[e(t_z)\left\langle J_i \| \hat{O}_2(\vec{r},t_z) \| J_i \right\rangle_{\mathrm{MS}} + e\left\langle J_i \| \Delta\hat{O}_2(\vec{r},t_z) \| J_i \right\rangle_{\mathrm{CP}} \right] \quad (5)$$

Similarly, the CP electric matrix element is expressed as the sum of the products of the one-body density matrix (OBDM) times the single-particle matrix elements,

$$\left\langle J_i \| \Delta\hat{O}_2(\vec{r},t_z) \| J_i \right\rangle = \sum_{jj'} OBDM(J_i, J=2, t_z, j, j')\left\langle j \| \Delta\hat{O}_2(\vec{r},t_z) \| j' \right\rangle \quad (6)$$

The single- particle matrix element of the CP term is

$$\left\langle j \| \Delta\hat{O}_J \| j' \right\rangle = \left\langle j \| \hat{O}_J \frac{\hat{Q}}{E_i - H_0} \mathrm{V}_{res} \| j' \right\rangle + \left\langle j \| \mathrm{V}_{res} \frac{\hat{Q}}{E_f - H_0} \hat{O}_J \| j' \right\rangle \quad (7)$$

where the operator $\hat{Q}$ is the projection operator onto the space outside the model space. The single particle core-polarization terms given in Eq.(7) are written as [11]

$$\left\langle j \| \Delta\hat{O}_J \| j' \right\rangle = \sum_{j_1 j_2 \lambda} \frac{(-1)^{j'+j_2+\lambda}}{\varepsilon_{j'} - \varepsilon_j - \varepsilon_{j_1} + \varepsilon_{j_2}} (2\lambda+1) \begin{Bmatrix} j & j' & J \\ j_2 & j_1 & \lambda \end{Bmatrix} \sqrt{(1+\delta_{j_1 j})(1+\delta_{j_2 j'})} \times \left\langle j j_1 | \mathrm{V}_{res} | j' j_2 \right\rangle_\lambda \left\langle j_2 \| \hat{O}_J \| j_1 \right\rangle \quad (8)$$

+terms with j_1 and j_2 exchanged with an overall minus sign,
where the index j_1 runs over particle states and j_2 over hole states and ε is the single-particle energy.

For the residual two-body interaction V_{res}, the two-body Michigan three range Yukawa (M3Y) interaction of Bertsch et al. [12] is adopted, where the two-body interaction can be used which is not restricted to a specific shell.

The quadrupole moment can be represented in terms of only the model space matrix elements by assigning effective charges($e^{eff}(t_z)$) to the protons and neutrons which are active in the model space,

$$Q(J=2) = \begin{pmatrix} J_i & 2 & J_i \\ -J_i & 0 & J_i \end{pmatrix} \sqrt{\frac{16\pi}{5}} \sum_{t_z} e^{eff}(t_z) \left\langle J_i \| \hat{O}_2(\vec{r}, t_z) \| J_i \right\rangle_{\mathrm{MS}} \quad (9)$$

The effective nucleon charge can be obtained as follows

$$e^{eff}(t_z) \left\langle J_i \| \hat{O}_2(\vec{r}, t_z) \| J_i \right\rangle_{\mathrm{MS}} = e(t_z) \left\langle J_i \| \hat{O}_2(\vec{r}, t_z) \| J_i \right\rangle_{\mathrm{MS}} + e \left\langle J_i \| \Delta\hat{O}_2(\vec{r}, t_z) \| J_i \right\rangle_{\mathrm{CP}} \quad (10)$$

$$e^{eff}(t_z) = e(t_z) + \frac{\left\langle J_i \| \Delta\hat{O}_2(\vec{r}, t_z) \| J_i \right\rangle_{\mathrm{CP}}}{\left\langle J_i \| \hat{O}_2(\vec{r}, t_z) \| J_i \right\rangle_{\mathrm{MS}}} e = e(t_z) + e\delta e(t_z) \quad (11)$$

where $\delta e(t_z)$ is the nucleon polarization charge.

Results and discussion

Shell model calculations are performed with NuShellX [13] with the *sd* model space for neutron number $N \leq 20$, which covered the orbits $1d_{5/2}$, $2s_{1/2}$ and $1d_{3/5}$ and *sdpf* model space for $N > 20$. Results based on the *sd*-shell interactions USDB (universal *sd*-shell interaction B) for *sd*-shell model space [14] and the *sdpf* interaction *sdpf-u* [15] for *sdpf* model space with valence (active) protons are restricted to the *sd* shell and *N*-20 neutrons to the *pf* shell. The 20 neutrons are frozen in *s*, *p* and *sd*-shells (full *sd* valence space for *Z*-8 protons and full *pf* valence space for *N*-20 neutrons).

The $2s1d$ shell interaction USDB used on this work is based on the derivation of the USD Hamiltonian [16] which has been refined with an updated and complete set of energy data. The Hamiltonian USDB leads to a new level of precision for realistic shell model wave functions. The radial wave functions for the single-particle matrix elements are calculated with the

harmonic oscillator (HO) potential. The size parameters b are calculated for each nucleus with mass number A as

$$b = \sqrt{\frac{\hbar}{M_p \omega}}, \quad \text{with}$$

$\hbar\omega = 45A^{-1/3} - 25A^{-2/3}$ [4]. The root mean square (rms) charge radius is calculated for each isotope, using HO single particle states and compared with the available experimental data of Ref. [17], and presented in tables 1-7, for each isotope considered in the present work. Microscopic perturbed calculations have been performed to include configurations excluded by the model space which incorporate one-particle-one-hole excitation from the core and the model space orbits into all higher orbits with $2\hbar\omega$ excitation. Effective charges for the model space protons and neutrons are obtained as given in Eq. (11). Calculations for the Q moments are presented for isotopes with $Z \geq 13$ and compared with the available experimental data given in Ref. [18] (the most recent data). No sign is given if it was not determined by experiment.

1. $_{13}$Al isotopes

The quadrupole moments are calculated for Al isotopes with mass number A = 23, 25, 26, 27, 28, 31, 32, 33 and with neutron number N = 10, 12, 13, 14, 15, 18, 19, 20, respectively. The proton and neutron effective charges are calculated according to Eq.(11) and tabulated in Table 1. The effective charges for the isotopes of mixed isoscalar- isovector states ($T_i \neq 0$) are nearly equal each other as can be seen from Table 1. For pure isoscalar ($T_i = 0$), the proton and neutron polarization charges $\delta e(t_z)$ are $0.34e$. The calculated quadrupole moments using these effective charges are all in a good agreement with the experimental data of Ref. [18], except ^{25}Al isotope, where the calculated value underestimates the measured value by about a factor of 1.4. The discrepancy between the theoretical and experimental results of the Q moment for ^{25}Al indicates a large deformation of this isotope which needs further research. The calculated and measured Q moments are shown in Fig. 1 as a function of neutron number N.

Table 1: Quadrupole moments in units of $e\,fm^2$ calculated with harmonic oscillator (HO) potential for Aluminum (Al) isotopes (Z = 13). Effective charges are obtained from core-polarization calculations. Experimental quadrupole moments are taken from Ref. [18].

A, N $_{13}$Al	J_i^π	$b(fm)$	rms $_{theo.}$	rms $_{exp.}$	e_p	e_n	$Q_{theo.}$	$Q_{exp.}$
23, 10	$5/2^+$	1.805	3.075		1.21	0.44	15.27	16±5
25, 12	$5/2^+$	1.825	3.102		1.19	0.48	17.05	24±2
26, 13	5^+	1.834	3.114		1.34	0.34	25.51	+26±3
27, 14	$5/2^+$	1.843	3.126	3.061	1.20	0.49	15.01	+14.02±1.0
28, 15	3^+	1.851	3.141		1.19	0.49	15.52	+17.2±1.2
31, 18	$5/2^+$	1.876	3.188		1.20	0.48	14.15	13.4±2.0
32, 19	1^+	1.884	3.200		1.20	0.49	2.52	2.5±.2
33,20	$5/2^+$	1.891	3.211		1.18	0.46	10.96	13.2±1.6

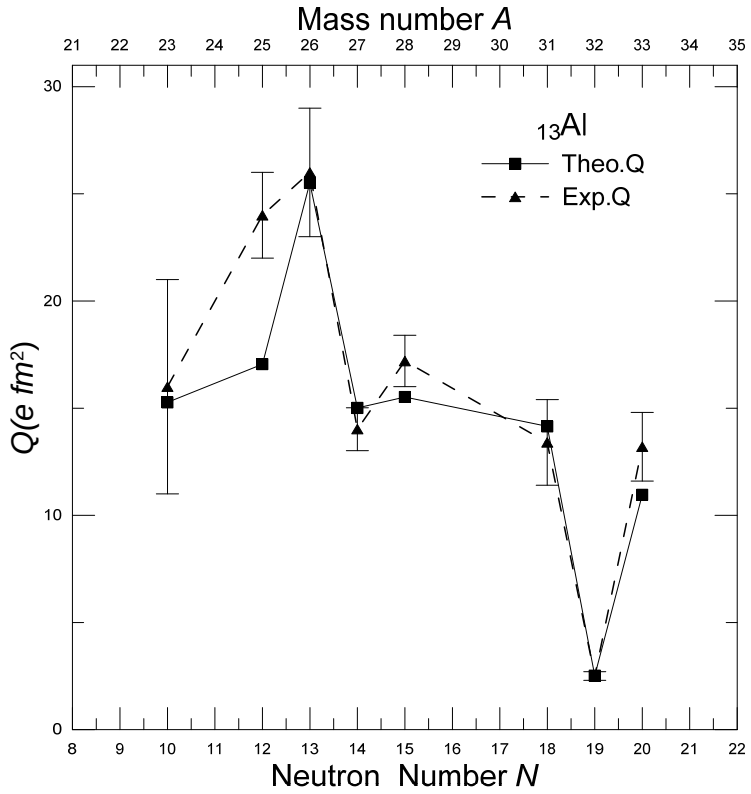

Fig. 1: Experimental [18] and theoretical quadrupole moments versus neutron number for Al isotopes.

2. $_{14}$Si isotopes

The quadrupole moments are calculated for Si isotopes with mass number A = 27, 28, 30, 42 and with neutron number N = 13, 14, 16, 28. The results of the Q moments are displayed in Table 2 in comparison with the experimental values. The Q moment for ^{28}Si (T_i = 0) agree very well with the experimental data, while for $T_i \neq 0$ isotopes, the calculated values overestimate the measured values. The calculated and measured Q moments are shown in Fig. 2 as a function of neutron number N. For A = 42 (N = 28), no experimental value is available, and the calculated Q moment is 17.68 $e\ fm^2$. This value shows a large prolate deformation for N = 28 closure, which indicates the drastic shape change when protons are removed away from the Z = 20 isotone ^{48}Ca. This is value is close to that of Ref. 1, with effective charges 1.35e and 0.35e, for the proton and neutron, respectively. Our calculated effective charges for this isotope are $e_{\mathrm{p}}^{\mathrm{eff}} = 1.28e$ and $e_{\mathrm{n}}^{\mathrm{eff}} = 0.35e$.

Table 2: Quadrupole moments in units of $e\,fm^2$ calculated with harmonic oscillator (HO) potential for Silicon (Si) isotopes (Z = 14). Effective proton and neutron charges are deduced from the core polarization calculation. Experimental quadrupole moments are taken from Ref. [18].

A, N $_{14}$Si	J_i^{π}	$b(fm)$	rms $_{\mathrm{theo.}}$	rms $_{\mathrm{exp.}}$	e_p	e_n	$Q_{theo.}$	$Q_{exp.}$
27, 13	$5/2^+$	1.843	3.162		1.2	0.49	12.21	6.3±1.4
28, 14	2^+	1.851	3.173	3.122	1.35	0.35	17.78	+16±3
30, 16	2^+	1.868	3.205	3.134	1.11	0.38	1.75	-5±6
42,28	2+	1.953	3.318		1.28	0.35	17.68	

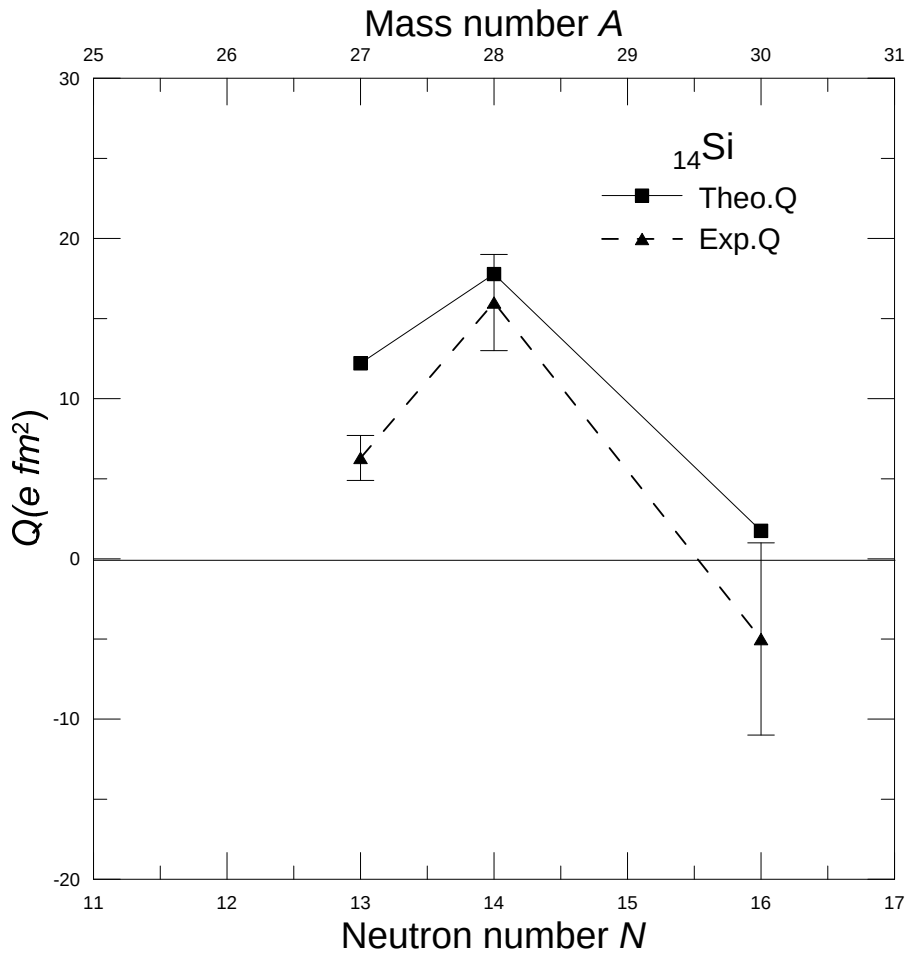

Fig. 2: Experimental [18] and theoretical quadrupole moments versus neutron number for Si isotopes.

3. $_{15}$P isotopes

Experimental Quadrupole moment is available only for mass number A = 28, which is equal to 13.7±1.4 $e\ fm^2$ [18]. The calculated value is 12.8 $e\ fm^2$, using HO, which is in an excellent agreement with the experimental data (Table 3). The calculated and measured Q-moments are shown in Fig. 3 as a function of neutron number N.

Table 3: Quadrupole moments in units of $e\ fm^2$ calculated with harmonic oscillator (HO) potential for Phosphorus (P) isotopes (Z = 15). Effective proton and neutron charges are deduced from the core polarization calculation. Experimental quadrupole moments are taken from Ref. [18].

A, N $_{15}$P	J_i^π	$b(fm)$	rms $_{theo.}$	rms $_{exp.}$	e_p	e_n	$Q_{theo.}$	$Q_{exp.}$
28, 13	3^+	1.851	3.199	3.189	1.19	0.5	12.8	13.7±1.4

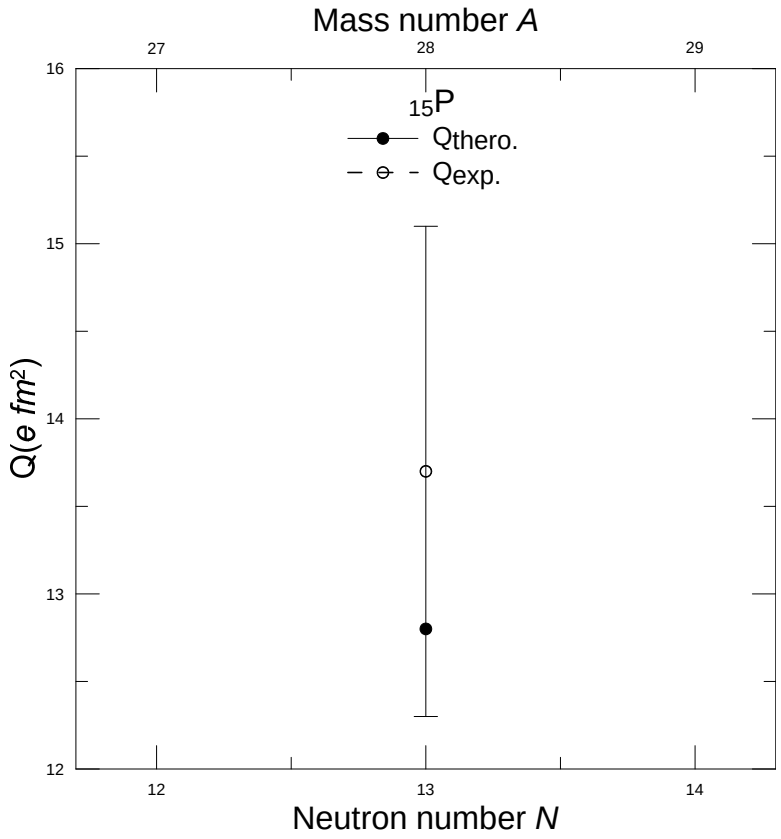

Fig. 3: Experimental [18] and theoretical quadrupole moments versus neutron number for P isotopes.

4. $_{16}$S isotopes

The quadrupole moments are calculated for S isotopes with mass number A = 32, 33, 34, 35, 43, 44 and with neutron number N = 16, 17, 18, 19, 27, 28. Calculations are performed with *sd*-shell model space for $N \leq 20$. The calculated effective charges for $T_i = 0$ (^{32}S) are 1.32e and 0.32e for the proton and neutron respectively. The experimental data are very well reproduced for all isotopes, except for ^{32}S (T_i = 0), where the calculated Q moment underestimates the measured value by about a factor of 1.5. The results of the Q moments are displayed in Table 4 in comparison with the experimental values, and plotted in Fig. 4 as a function of neutron number N. For A = 43, the neutron number N = 27. So, calculations are performed with *sdpf* model space with the interaction while the remaining seven neutrons are distributed over *pf*-shell orbits. The calculated Q = 23.31 e fm^2 which agrees very well with the measured one, 23±3 e fm^2. For the neutron-rich ^{44}S isotope with N = 28, *sdpf* model space with the configuration $\pi(sd)^8$, 12 frozen neutrons occupy the *sd* shell and $\nu(fp)^8$ gives the value -15.84 e fm^2 for the Q moment of the first excited 2^+ state, which agree with the theoretical value -16 e fm^2 of Ref. [1] using *sdpf-u* interaction [15] with effective charges 1.35e and 0.35e, for the protons and neutrons, respectively. No experimental value is available for this isotope. The large value of Q moment for this even-even isotope indicates that ^{44}S is a deformed nucleus. This is supported by the large $B(E2)$ value and small 2_1^+ energy [1]. The calculated proton and neutron effective charges for cross-shell *sd-pf* nuclei are less than those of *sd*-shell nuclei.

Table 4: Quadrupole moments in units of $e\,fm^2$ calculated with harmonic oscillator (HO) potential for Sulfur (S) isotopes (Z = 16). Effective proton and neutron charges are deduced from the core polarization calculation. Experimental quadrupole moments are taken from Ref. [18].

A, N $_{16}$S	J_i^π	$b(fm)$	rms $_{theo.}$	rms $_{exp.}$	e_p	e_n	$Q_{theo.}$	$Q_{exp.}$
32, 16	2^+	1.884	3.277	3.261	1.32	0.32	-10.55	-16±2
33, 17	$3/2^+$	1.891	3.290		1.2	0.48	-6.31	-6.78±1.3
34, 18	2^+	1.899	3.305	3.285	1.2	0.48	4.0	+4±3
35, 19	$3/2^+$	1.906	3.316		1.17	0.49	4.92	+4.7±1.3
43, 27	$7/2^-$	1.959	3.382		1.34	0.29	23.31	23±3
44, 28	2^+	1.966	3.391		1.25	0.38	-15.84	

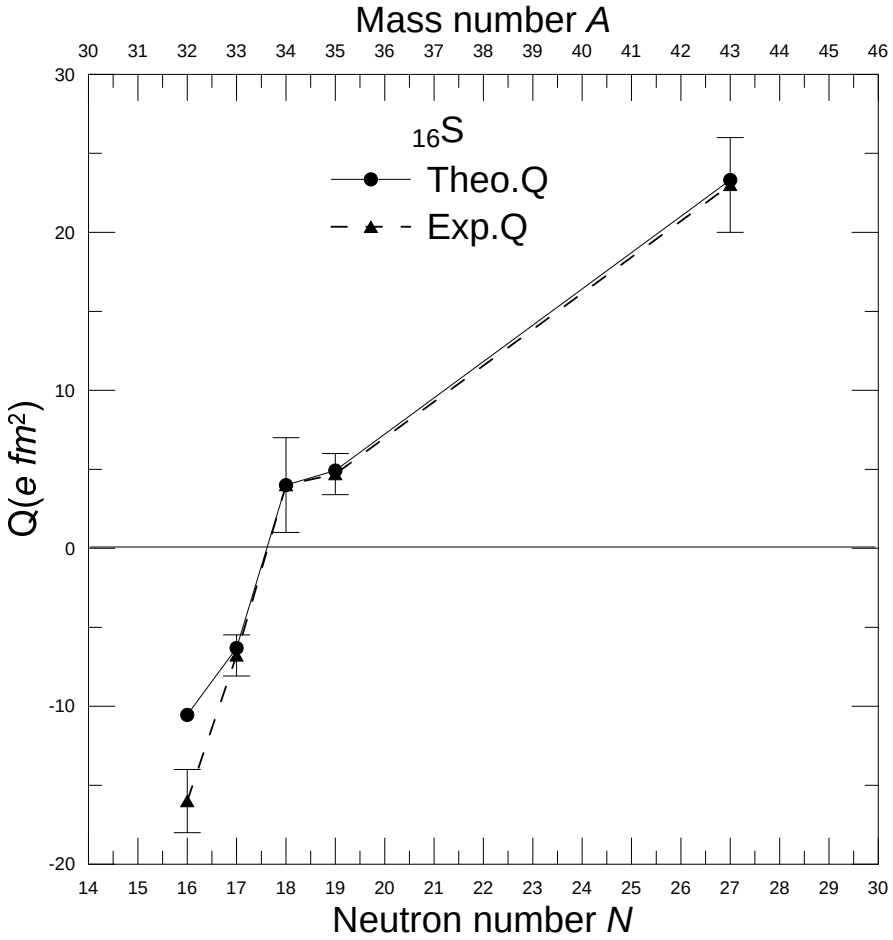

Fig. 4: Experimental [18] and theoretical quadrupole moments versus neutron number for S isotopes.

5. $_{17}$Cl isotopes

The quadrupole moments are calculated for Cl isotopes with mass number A = 35, 36, 37 and with neutron number N =18, 19, 20. The results of the Q moments are displayed in Table 5 in comparison with the experimental values. The calculated and measured Q moments are shown in Fig. 5 as a function of neutron number N. The data are very well reproduced and confirm the oblate character of these isotopes.

Table 5: Quadrupole moments in units of $e\,fm^2$ calculated with harmonic oscillator (HO) potential for Chlorine (Cl) isotopes (Z = 17). Effective proton and neutron charges are deduced from the core polarization calculation. Experimental quadrupole moments are taken from Ref. [18].

A, N $_{17}$Cl	J_i^π	$b(fm)$	rms $_{theo.}$	rms $_{exp.}$	e_p	e_n	$Q_{theo.}$	$Q_{exp.}$
35, 18	$3/2^+$	1.906	3.335	3.365	1.19	0.48	-8.15	-8.5±1.1
36,19	2^+	1.913	3.347		1.22	0.37	-1.27	-1.8±0.4
37, 20	$3/2^+$	1.920	3.358	3.384	1.2	0.48	-6.85	-6.44±0.7

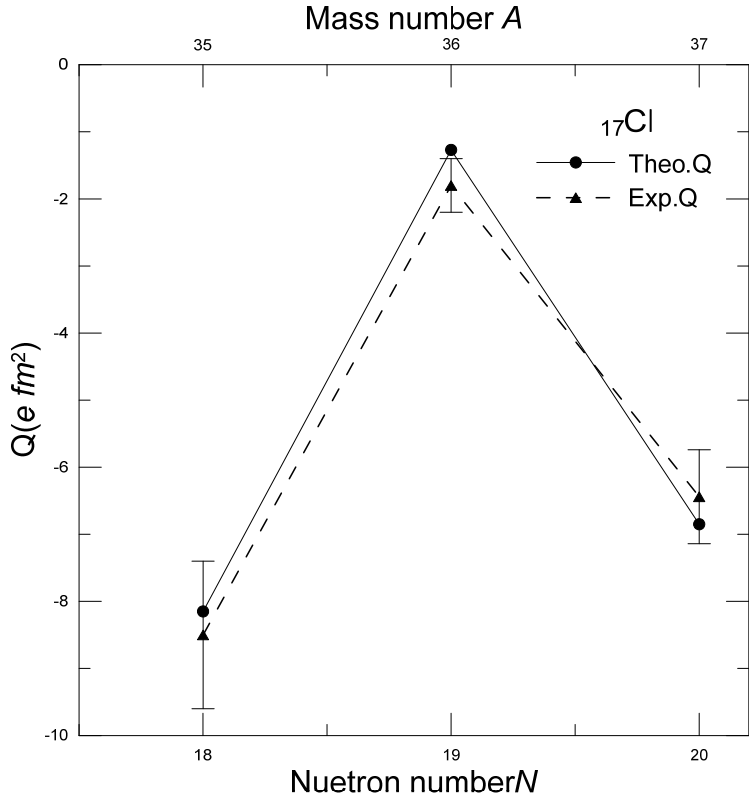

Fig. 5: Experimental [18] and theoretical quadrupole moments versus neutron number for Cl isotopes.

6. $_{18}$Ar isotopes

The quadrupole moments are calculated for Ar isotopes with mass number A = 35, 36, 37 and neutron number N = 17, 18, 19 using *sd*-shell model. The calculated values agree very well with the measured values and confirm the oblate character of ^{35}Ar isotope. For A = 39, 40, 41, 43, 44, 46 and with neutron number, 21, 22 23, 25, 26, 28, the cross *sdpf*- shell model is used with *N*-8 active protons are distributed over *sd*-shell orbits. The *N*-20 neutrons are distributed over the *pf*-shell orbits with 12 frozen neutrons in *sd*-shell orbits. The results of the Q moments are displayed in Table 6 in comparison with the experimental values. The calculated values for ^{39}Ar and ^{41}Ar isotopes agree very well with the measured values and confirm the oblate character of these isotopes. The configuration used for the neutron rich nuclei (N > 20) gives the value -2.64 *e fm*^{2} for the Q moment of the first excited 2^+ state of ^{44}Ar, in comparison with the experimental value -8 *e fm*^{2}. This value indicates a small oblate deformation. This value agrees with other theoretical models of Ref. [1], where they used e_p = 1.5e and e_n = 0.5e. For ^{46}Ar, N = 28 (magic number),

our calculation shows that the values for the Q moment are 16.75 $e\ fm^2$ which show a large prolate deformation than the small oblate deformation of ^{44}Ar. The results of the Q moments are displayed in Table 6 in comparison with the experimental values and plotted in Fig. 6 as a function of neutron number N.

Table 6: Quadrupole moments in units of $e\ fm^2$ calculated with harmonic oscillator (HO) for Argon (Ar) isotopes (Z = 18). Effective proton and neutron charges are deduced from the core polarization calculation. Experimental quadrupole moments are taken from Ref. [18].

$A,\ N$ $_{18}$Ar	J_i^π	$b(fm)$	rms $_{theo.}$	rms $_{exp.}$	e_p	e_n	$Q_{theo.}$	$Q_{exp.}$
35, 17	$3/2^+$	1.906	3.350	3.364	1.19	0.48	-8.42	-8.4±1.5
36, 18	2^+	1.913	3.364	3.391	1.32	0.32	12.44	+11±6
37, 19	$3/2^+$	1.921	3.377	3.391	1.21	0.46	7.50	+7.6±0.9
39, 21	$7/2^-$	1.934	3.395	3.409	1.31	0.25	-11.79	-12±3
40, 22	2+	1.941	3.404	3.427	1.05	0.53	6.85	+1±0.4
41, 23	$7/2^-$	1.947	3.412	3.425	1.26	0.33	-3.64	-4.2±0.4
43, 25	$5/2^-$	1.960	3.428	3.441	1.18	0.35	8.8	+14.2±1.4
44, 26	2^+	1.966	3.436	3.445	1.13	0.34	-2.64	-8[a]
46, 28	2^+	1.978	3.451	3.438	1.39	0.26	16.75	

[a] Ref. [1].

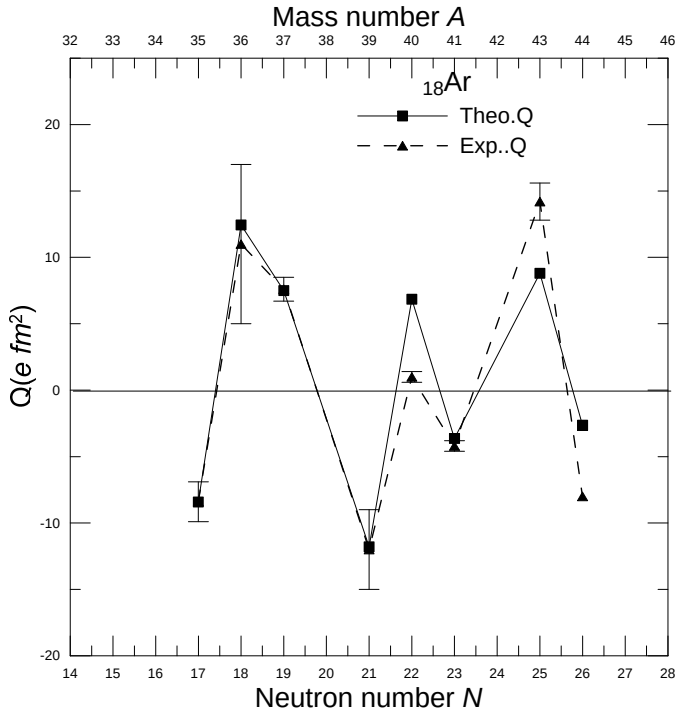

Fig. 6: Experimental [18] and theoretical quadrupole moments versus neutron number for Ar isotopes.

7. $_{19}$K isotopes

The quadrupole moments are calculated for K isotopes with mass number A = 37, 39 and neutron number N = 18, 19 using *sd*-shell model. For A = 40, 41 and neutron number 21, 22, the cross *sdpf*- shell model is used with N-8 active protons are distributed over *sd*-shell orbits. The N-20 neutrons are distributed over the *pf*-shell orbits with 12 frozen neutrons in *sd*-shell orbits. The results of the Q moments are

displayed in Table 7 in comparison with the experimental values. The calculated values for ^{39}K, ^{40}K agrees very well with the measured values and within the experimental error for ^{37}K. The calculated and measured Q moments are shown in Fig. 7 as a function of neutron number N.

Table 7: Quadrupole moments in units of $e\,fm^2$ calculated with harmonic oscillator (HO) potential for Potassium (K) isotopes (Z = 19). Effective proton and neutron charges are deduced from the core polarization calculation. Experimental quadrupole moments are taken from Ref. [18].

A, N $_{19}$K	J_i^π	$b(fm)$	rms $_{theo.}$	rms $_{exp.}$	e_p	e_n	$Q_{theo.}$	$Q_{exp.}$
37, 18	$3/2^+$	1.921	3.394		1.21	0.46	6.90	10.6±4
39, 20	$3/2^+$	1.934	3.415	3.345	1.20	0.48	6.28	6±2
40, 21	4^-	1.941	3.427	3.438	1.18	0.30	-6.35	-7.5±2
41, 22	$3/2^+$	1.947	3.432	3.452	1.36	0.23	6.85	7.11±0.7

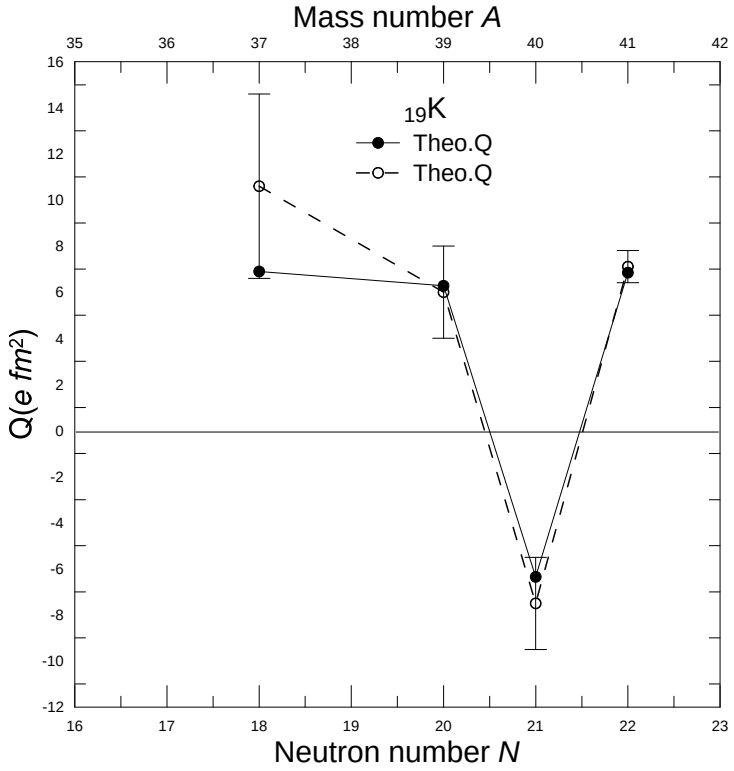

Fig. 7: Experimental [18] and theoretical quadrupole moments versus neutron number for K isotopes.

Comparison of measured and calculated quadrupole moments is shown in Fig. 8 for all isotopes considered in this work. The line represents Q_{theo}= Q_{exp}. From all the figures presented above one can see that good agreement is obtained with the measured data for most of the isotopes while it deteriorates for some other where they need further investigation.

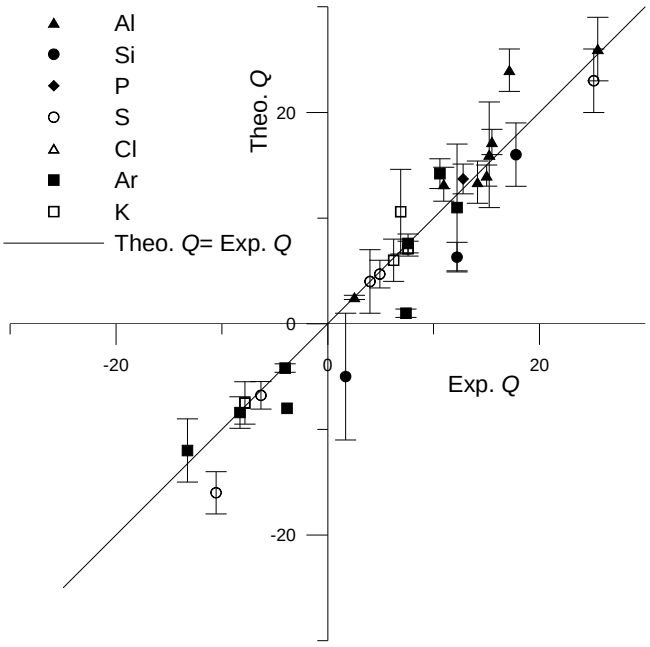

Fig. 8: Comparison of measured and calculated quadrupole moments. The line represents $Q_{theo}=Q_{exp}$.

Conclusions

Shell-model calculations are performed for *sd* and cross *sd-pf* shell isotopes with $Z \geq 13$, including core-polarization effects through first order perturbation theory, where 1p-1h with $2\hbar\omega$ excitation are taken into considerations. Effective charges for all $T_i \neq 0$ *sd*-shell isotopes are nearly equal each other. For $T_i = 0$ isotopes, the polarization charges are in the range 0.31*e* to 0.35*e*. The calculated proton and neutron effective charges for cross-shell *sd-pf* nuclei are less than those of *sd*-shell nuclei. Average isovector effective charges for *sd*-shell nuclei are 1.19*e*, 0.47*e*, for the proton and neutron, respectively. Average isoscalar polarization charge is 0.33*e*. For cross-shell *sd-pf* nuclei, the average isovector effective charges are found to be equal to 1.24*e* and 0.34*e*, for the proton and neutron, respectively. Good agreement is obtained with the measured data for most of the isotopes considered in this work while it deteriorates for some of them and need further investigation.

References

[1] Kazunari Kaneko, Yang Sun, Takahiro Mizusaki, Munetake Hasegawa, Phys. Rev. C 83 (2011) 014320.

[2] L. Gaudefroy, J. M. Daugas, M. Hass, S. Grévy, Ch. Stodel, J. C. Thomas, L. Perrot, M. Girod, B. Rossé, J. C. Angélique, D. L. Balabanski, E. Fiori, C. Force, G. Georgiev, D. Kameda, V. Kumar, R. L. Lozeva, I. Matea, V. Méot, P. Morel, B. S. Nara Singh, F. Nowacki, and G. Simpson, Phys. Rev.Lett. 102 (2009) 092501.

[3] O. Sorlin, Zs. Dombrádi, D. Sohler, F. Azaiez, J. Timár, Yu. -E. Penionzhkevich, F. Amorini, D. Baiborodin, A. Bauchet, F. Becker, M. Belleguic, C. Borcea, C. Bourgeois, Z. Dlouhy, C. Donzaud, J. Duprat, L. Gaudefroy, D. Guillemaud-Mueller, F. Ibrahim, M. J. Lopez, R. Lucas, S. M. Lukyanov, V. Maslov, J. Mrazek, C. Moore, F. Nowacki, F. PougheonAffiliated with Institut de Physique Nucléaire, IN2P3-CNRS, M. G. Saint-Laurent, F. Sarazin, J. A. Scarpaci, G. Sletten, M. Stanoiu, C.

Stodel, M. Taylor, Ch. Theisen, Eur. Phys. J. A. 22 (2004) 173-178.
[4] B. A. Brown, R. Radhi, B. H. Wildenthal, Phys. Rep. 101 (1983) 313.
[5] H. Sagawa, B. A. Brown, Nucl. Phys. A 430 (1984) 84.
[6] W. A. Richter, S. Mkhize, B. Alex Brown, Phys. Rev. C 78 (2008) 064302.
[7] M.De Rydt, G. Neyensa, K. Asahi, D. L. Balabanski, J. M.Daugas, M. Depuydt, L. Gaudefroy, S.Grevy, Y. Hasama, Y. Ichikawa, P. Moreld, T. Nagatomo, T. Otsukai, L. Perrot, K. Shimada, C. Stodel, J. C. Thomas, H. Ueno, Y. Utsuno, W. Vanderheijden, N. Vermeulen, P. Vingerhoets, Yoshimi, Phys. Lett. B 678 (2009) 334.
[8] M. De Rydt, M. Depuydt, G. Neyens, Atomic Data and Nuclear Data tables 99 (2013) 391.
[9] R. A. Radhi, Z. A. Dakhil, N. S. Manie, Eur. Phys. J. A 50 (2014) 115.
[10] R. A. Radhi, E. A. Salman, Nucl. Phys. A 806, (2008) 179.
[11] P. J. Brussaard, P. W. M. Glaudemans, Shell Model ApplicationsIn Nuclear Spectroscopy (1977) (Amsterdam: North Holand).
[12] G. Berstch, J. Borysowicz, H. McManus, W. G. Love, Nucl. Phys. A 284 (1977) 399.
[13] B. A. Brown, W. D. M. Rae, Nuclear Data Sheet 120 (2014) 115.
[14] B. Alex Brown, W. A. Richter, Phys. Rev. C 74 (2006) 034315.
[15] F. Nowacki, A. Poves, Phys. Rev. C 79 (2009) 014310.
[16] B. A. Brown, B. H. Wildental, Annu. Rev. Nucl. Part. Sci. 38 (1988) 29.
[17] I. Angeli, K. P. Marino, Atomic Data and Nuclear Data Tables, 99 (2013) 69.
[18] N. J. Stone, Table of nuclear magnetic dipole and electric quadrupole moments, International Data Committee, International Atomic Energy Agency (IAEA), INDC (NDS) (2014) 0658.